RESEARCH PAPER

Development And Evaluation Of Fluconazole Loaded Ethosomal And Liposomal Gels For Enhanced Antifungal Therapy

Apoorva Tiwari*, Sachin K Jain, Sudha Vengurlekar
Faculty of Pharmacy, Oriental University Indore, MP
Corresponding Author – apoorvatiwari2010@gmail.com

ABSTRACT
The present study focused on the development and evaluation of fluconazole-loaded ethosomal and liposomal gels for enhanced topical antifungal delivery. Preformulation studies confirmed the purity and suitability of fluconazole for vesicular formulation, with a melting point of 139°C, partition coefficient of 0.57, and characteristic FTIR peaks confirming drug identity and compatibility with excipients.
Ethosomal and liposomal formulations were optimized using Taguchi design and intensive grid search methodology. Among ethosomal formulations, EF2 was selected as the optimized batch, exhibiting vesicle size of 368.4 nm and entrapment efficiency of 85.50%. The optimized liposomal formulation LF3 showed vesicle size of 320.4 nm and entrapment efficiency of 76.91%. Incorporation of optimized vesicles into carbopol gel base produced smooth, homogeneous gels with acceptable pH, viscosity, spreadability, and drug content suitable for topical application. In-vitro diffusion studies demonstrated sustained and enhanced drug release from both vesicular gels, with ethosomal gel showing comparatively greater permeation due to the presence of ethanol and flexible phospholipid vesicles. Stability studies conducted under accelerated conditions revealed no significant changes in physical appearance, pH, drug content, vesicle size, or entrapment efficiency, confirming formulation stability. Antifungal activity studies showed larger zones of inhibition for the ethosomal and liposomal gels compared with conventional fluconazole gel, indicating improved antifungal efficacy.
Overall, the optimized ethosomal gel demonstrated superior drug permeation, higher entrapment efficiency, enhanced antifungal activity, and better therapeutic performance compared with the liposomal gel, suggesting its potential as an effective topical carrier system for fluconazole delivery in fungal infections.

Keywords: Fluconazole, Ethosomal gel, Liposomal gel, Antifungal therapy, Topical delivery, Vesicular formulation.
How to cite this article: Tiwari A, Jain SK, Vengurlekar S. Development And Evaluation Of Fluconazole Loaded Ethosomal And Liposomal Gels For Enhanced Antifungal Therapy. Int J Drug Deliv Technol. 2026;16(59s): 293-307-. DOI: 10.25258/ijddt.16.59s.28
Source of support: Nil
Conflict of interest: None

INTRODUCTION

Topical drug delivery systems are widely used for the treatment of fungal infections because they deliver the drug directly to the site of action, minimize systemic exposure, and reduce adverse effects associated with oral therapy. Conventional topical formulations of fluconazole such as creams and ointments often suffer from poor skin penetration, inadequate drug retention, and frequent application requirements, which may reduce therapeutic effectiveness and patient compliance. Hence, the development of advanced topical gel systems capable of improving skin permeation and providing controlled drug release has gained considerable attention in pharmaceutical research.

Vesicular carrier systems such as ethosomes and liposomes have emerged as promising approaches for topical and transdermal drug delivery. Ethosomes are phospholipid vesicles containing high concentrations of ethanol, which enhance vesicle flexibility and improve drug permeation through the stratum corneum by disrupting skin lipids. Liposomes are phospholipid bilayer vesicles that enhance drug localization, improve stability, and provide sustained drug release at the site of application. Incorporation of these vesicular systems into gel formulations combines the advantages of improved permeation, controlled drug release, prolonged skin retention, enhanced stability, and ease of topical application.

Fluconazole is a broad-spectrum triazole antifungal agent widely used for the treatment of superficial fungal infections such as candidiasis and dermatophytosis. However, its topical delivery is limited by poor penetration into deeper skin layers. Therefore, the present study was undertaken to develop and evaluate fluconazole-loaded ethosomal and liposomal gels with the objective of enhancing skin permeation, improving antifungal activity, and

achieving sustained drug release for better therapeutic efficacy and patient compliance.

MATERIALS AND METHODS

Preparation of Gels: Preparation of carbopol gel base: Carbopol 934 (0.5 g) was dispersed in water under gentle agitation and left to hydrate and swell for 24 hours to prepare the 0.5% gel base. Glycerin (2 ml) was subsequently added to achieve appropriate gel consistency (Table 1). The same procedure was applied to prepare 1% and 2% carbopol gel bases (Chung et al., 2002; Nair, 2017).

Table 1: Composition of different gel base

Formulation	Carbopol (%)
EF1	0.5
EF2	1.0
EF3	2.0

Preparation of ethosomal gels: 1 gm of the ethosomal formulation was dispersed in 10 ml ethanol and centrifuged at 6000 rpm for 20 minutes to separate unentrapped drug. The supernatant was carefully removed by decantation, and the sediment containing the ethosomes was incorporated into the carbopol gel base (Table 2).

Table 2: Composition of optimized ethosome formulation

Formulation	SPC (%w/v)	Ethanol (%w/v)	Propylene Glycol (%w/v)
EF1	3	43	10

The ethosomal sediment was blended into the gel base using a mechanical stirrer at 25 rpm for 10 minutes to ensure homogeneous distribution. The optimized ethosomal formulation was incorporated into gel bases at concentrations of 0.5%, 1%, and 2% w/w (Katare et al., 1991; Mallesh et al., 2012).

Preparation of liposomal gels: 1 gm of the liposomal preparation was dispersed in 10 ml ethanol and centrifuged at 6000 rpm for 20 minutes to isolate the vesicular fraction. The supernatant was decanted, and the sediment was transferred into the carbopol gel base for incorporation (Table 3).

Table 3 Composition of optimized liposome formulation

Formulation	Lecithin (mg)	Cholesterol (mg)	Speed (rpm)
LF2	152	38.3	100

Incorporation of the liposomal fraction into the gel base was carried out using a REMI type BS mechanical stirrer at 25 rpm for 10 minutes. The optimized liposomal formulation was prepared at three gel concentrations: 0.5%, 1%, and 2% w/w (Katare OP et al., 1991; Khan et.al, 2024).

Evaluation of Gels

Determination of pH: Aliquots of 50 g of each gel formulation were transferred to a beaker and the pH was measured using a calibrated digital pH meter. For topical skin preparations intended to treat fungal infections, a pH range of 3–9 is considered acceptable (Bhalaria et al., 2009).

Spreadibility: Gel Spreadibility was evaluated using a modified two-glass-slide apparatus, based on the slip-and-drag principle. The lower slide was fixed to a wooden base while the upper slide was connected via a hook to a balance. The Spreadibility coefficient (S) was calculated using the formula S = ml/t, where m is the weight applied to the upper slide, l is the distance travelled, and t is the time taken to cover that distance. Mass and distance were held constant across measurements, with time as the variable parameter. Each formulation was measured in triplicate and the mean value reported (Sabale V., 2011).

Measurement of viscosity: The rheological properties of the gels were assessed using a Brookfield DV-II viscometer equipped with a T-Bar spindle mounted on a helipath stand to ensure consistent and reproducible readings.

Selection of spindle: Appropriate spindle selection was determined empirically, beginning with spindle T91 and progressing through higher-numbered spindles. The objective was to achieve a percentage torque reading between 10 and 100, with measurement precision increasing as the torque value approaches 100%. Spindle T95 was identified as most suitable and was used consistently for all gel viscosity measurements.

Spindle Immersion: The T-bar spindle (T95) was inserted vertically into the center of the gel sample, ensuring that the spindle tip did not contact the bottom of the container.

Measurement of Viscosity: Viscosity of each gel was measured using T-bar spindle T95. All experimental variables known to influence viscosity, including temperature, pressure, and sample volume, were maintained constant throughout the measurement process. The helipath mechanism traversed the spindle vertically through the sample, recording viscosity at multiple depth positions. A minimum torque reading of 10% was maintained. Five consecutive readings collected over 60 seconds were averaged to obtain the final viscosity value.

Drug content: One gram of the prepared gel was dissolved in 100 ml ethyl alcohol. The solution was filtered, and serial dilutions were prepared from the filtrate. Absorbance of each dilution was measured at 260 nm. Drug content was determined by linear regression analysis using the pre-established calibration curve (Pradhan et al., 2015).

In-vitro diffusion study: Drug release from the gel formulations was evaluated in a modified Franz diffusion cell assembly (Figure 1). A dialysis membrane (Hi Media, molecular weight cut-off 5000 Da) was mounted between the donor and receptor compartments. Ethosomal or liposomal gel equivalent to 500 mg fluconazole was loaded into the donor compartment, while the receptor compartment was filled with 24 ml of phosphate buffer pH 7.4. The apparatus was maintained at 37 ± 0.5°C with continuous stirring at 50 rpm. At predetermined time intervals, 5 ml aliquots were withdrawn from the receptor compartment through the side sampling port and analyzed for drug content by UV-Vis spectrophotometry.

Figure 1 Franz diffusion cell with membrane mounted between compartments

Stability studies: The optimized fluconazole-loaded ethosomal and liposomal gel formulations were subjected to accelerated stability evaluation at two storage temperatures: 4 ± 1°C and 28 ± 1°C (ambient). Formulations were stored in sealed, amber-colored glass vials at each condition. Physical and chemical stability was monitored by measuring vesicle size and drug content at 7, 14, 21, and 28 days.

Effect of storage temperature on vesicle size: Changes in vesicle size upon storage at 4 ± 1°C and 28 ± 1°C were monitored using a Malvern Zetasizer at predetermined intervals of 7, 14, 21, and 28 days.

Effect of storage temperature on drug content: Drug content of both formulations was determined after 7, 14, 21, and 28 days of storage. The drug remaining in the ethosomal and liposomal gel matrices was quantified spectrophotometrically to provide an indirect measure of vesicular drug retention under different storage conditions.

Antifungal Activity

Pathogenic fungus used: The fungal strains *Aspergillus niger* and *Candida albicans* employed in the antifungal activity studies were obtained from the Microbial Culture Collection (MCC), National Centre for Cell Science, Pune, Maharashtra, India.

Media preparation: Composition of nutrient agar media (Table 4) is given below:

Table 4. Composition of nutrient agar media

Potatoes extract	200 gms
Dextrose	20 gms
Agar	15 gms
Distilled Water	to make 1000ml
pH (at 25°C)	5.6±0.2

The agar medium was prepared by transferring all dry ingredients to a conical flask containing the required volume of distilled water, followed by heating with continuous stirring until complete dissolution was achieved. The prepared medium was then brought to a boil in a flask of adequate capacity.

Sterilization of culture media: The prepared medium in each flask was sealed with a cotton plug and autoclaved at 121°C (15 lbs/inch²) for 15 minutes to achieve complete sterilization.

Preparation of plates: Following sterilization, the molten agar was promptly dispensed into sterile Petri dishes (approximately 20 ml per plate) on a level surface. The poured plates were allowed to solidify at room temperature and then incubated overnight at 37°C to verify sterility prior to use. Plates were dried at 50 ± 0.5°C for 30 minutes before inoculation.

Revival of the microbial cultures: Lyophilized microbial cultures were rehydrated under aseptic conditions by inoculation into sterile nutrient broth and, for fungal strains, into potato dextrose broth. Cultures were incubated at 37 ± 0.5°C for 24 hours until turbidity indicated active growth. Subcultures were then streaked onto nutrient agar and potato dextrose agar plates and re-incubated under the same conditions for 24 hours to establish pure isolates. Confirmed cultures were stored at 4°C as working stock preparations for subsequent experiments.

Antimicrobial sensitivity: Antifungal sensitivity testing was performed to evaluate the activity of each gel formulation against the study organisms. Whatman filter paper discs (6 mm diameter) were impregnated with a 100 mg/ml drug stock solution

and air-dried under aseptic conditions. Potato dextrose agar plates were seeded with the respective fungal organism by the spread-plate technique and left for 5 minutes. Drug-loaded discs were then placed at the center of the inoculated plates, which were subsequently incubated at 37 ± 0.5°C for 24 hours. The zones of inhibition were measured after incubation to assess sensitivity.

Antibiogram studies: Broth cultures of *Aspergillus niger* and *Candida albicans* isolates confirmed as susceptible at 100 mg/ml were prepared by inoculating a loopful of each culture into sterile nutrient broth and incubating at 37 ± 0.5°C for 48 hours. Lawn cultures were established by swabbing the broth cultures onto sterile nutrient agar and potato dextrose agar plates using sterile cotton swabs.

The paper disc diffusion method was applied to determine the antifungal activity of the gel formulations using a standardized protocol. Three concentrations—25, 50, and 100 mg/ml—were evaluated. Filter paper discs impregnated with each concentration were placed on the surface of pre-inoculated agar plates immediately after seeding. Direct use of undiluted overnight broth cultures or uncontrolled clinical material as inocula was avoided to ensure consistency and prevent mixed-culture interference. Plates were incubated at 37 ± 0.5°C for 48 hours and then examined for zones of inhibition around each disc.

Mathematical Modelling of Drug Release

Mathematical treatment of in-vitro release data: Quantitative interpretation of drug release profiles is facilitated by applying mathematical models that relate dissolution data to dosage form characteristics. The following kinetic models were applied to describe the release behaviour of fluconazole from the gel formulations.

Zero-order kinetics: This model describes formulations that release a constant quantity of drug per unit time, independent of drug concentration. It represents the ideal release profile for achieving sustained pharmacological effects over an extended period, and is expressed as:

$$Q_t = Q_o + K_o t$$

where Qt is the cumulative amount of drug released at time t, Qo is the initial drug amount in solution (typically Qo = 0), and Ko is the zero-order release rate constant (Bourne, 2002).

First-order kinetics: In this model, the rate of drug release is proportional to the remaining drug concentration and is expressed as:

$$\log Q_t = \log Q_o + \frac{K_1 t}{2.303}$$

where Qt is the amount of drug dissolved at time t, Qo is the initial drug amount, and K1 is the first-order release rate constant.

Higuchi model: Higuchi formulated a series of mathematical models to characterize the release of both water-soluble and sparingly soluble drugs from semi-solid and solid matrices, based on drug particles dispersed uniformly within a diffusion matrix. The simplified Higuchi equation is expressed as:

$$Q = K_H . t^{1/2}$$

where Q is the cumulative amount of drug released at time t and KH is the Higuchi dissolution constant. This model characterizes drug release as a Fickian diffusion process exhibiting a square-root-of-time dependence. It is applicable to a range of modified-release formulations, including transdermal systems and matrix tablets containing water-soluble drugs (Bruphy and Deasy, 1987; Higuchi, 1963).

Korsmeyer-Peppas model: Korsmeyer and colleagues proposed a semi-empirical power law equation to describe generalized drug release behavior from controlled-release polymer matrices:

$$\frac{M_t}{M_\infty} = a\, t^n$$

where Mt/M∞ represents the fractional drug release, a is a kinetic constant, t is time, and n is the diffusion exponent characterizing the transport mechanism. The n value is obtained from the slope of a log(Mt/M∞) versus log(t) plot (Korsmeyer et al., 1983). Peppas demonstrated that this equation adequately describes drug release from slabs, spheres, cylinders, and discs regardless of the underlying transport mechanism (Peppas et al., 1989). For a planar slab geometry, n = 0.5 indicates Fickian diffusion, n values between 0.5 and 1.0 indicate anomalous (non-Fickian) transport, and n = 1.0 corresponds to Case-II (zero-order) transport (Table 4.11).

$$\frac{M_{t-l}}{M_\infty} = a\,(t-l)^n$$

When there is the possibility of a burst effect, b, this equation becomes:

$$\frac{M_t}{M_\infty} = at^n + b$$

In the absence of lag time or burst release, the l and

b terms become zero, reducing the equation to the basic power law expression at^n. This Power Law model has been widely applied to characterize drug release from diverse modified-release pharmaceutical systems (Table 5) (Rinaki, 2003).

Table 5. Interpretation of diffusional release mechanisms.

Release exponent (*n*)	Drug transport mechanism	Rate as a function of time
0.5	Fickian diffusion	$t^{-0.5}$
0.5<*n*<1.0	Anomalous transport	t^{n-1}
1.0	Case-II transport	Zero-order release
Higher than 1.0	Super Case-II transport	t^{n-1}

RESULT & DISCUSSION

The gel was prepared and evaluated as -

Evaluation of Ethosomal Gel

Drug content: Drug content is a critical quality attribute of vesicular formulations. The ethosomal gels demonstrated satisfactory drug retention, with measured values ranging from 97.5 to 98.25%, confirming the effective entrapment capacity of the formulations.

pH: The pH of a transdermal formulation is a critical parameter for ensuring skin compatibility. All prepared ethosomal gels exhibited pH values in the range of 6.9–7.3, which falls within the skin-compatible range, confirming their suitability for topical administration.

5.4.3 Spreadibility: Spreadibility of the ethosomal gels was evaluated using a modified slip-and-drag apparatus. Recorded values ranged from 10.75 to 11.75 g/cm/sec, reflecting appropriate application characteristics. Formulations with excessively high or low Spreadibility would present challenges for uniform topical application.

Viscosity measurements: Gel viscosity was measured using a Brookfield DV-II viscometer equipped with a T-Bar spindle and helipath attachment. All environmental variables known to affect gel rheology, including temperature, pressure, and sample volume, were strictly controlled throughout measurement. Analyses were conducted at 25 degrees C, since elevated temperatures typically reduce gel viscosity. Shear rate and measurement duration were the only parameters varied. Samples were equilibrated to room temperature prior to analysis to avoid anomalously elevated viscosity readings resulting from cold-storage effects.

Spindle selection employed a sequential trial-and-error approach, beginning with T91 and progressing numerically until the % torque reading fell within the optimal range of 10–100, with precision improving near the upper bound. Spindle T95 was confirmed as appropriate for all gel samples. The helipath attachment allowed the T-Bar spindle to move vertically through the sample, recording viscosity at multiple positions. A mean value derived from five readings collected over 60 seconds was reported as the final viscosity.

Viscosity data for the liposomal gels confirmed a direct relationship between polymer concentration and measured viscosity. Increased viscosity at higher polymer concentrations is attributed to enhanced intermolecular cross-linking and network densification. The reduced proportion of free liquid in highly concentrated polymer matrices further contributes to increased flow resistance, necessitating greater shear stress to achieve a defined rate of deformation.

Table 6. Results of ethosomal formulations

Code	Drug content (%)	pH	Spreadibility (gm.cm/sec.)	Viscosity (cps)
EF1	98.25 ±0.027	6.9±0.021	11.75±0.075	6540.06±1.70
EF2	98.12 ± 0.021	7.2±0.040	11.08±0.042	9467.03±0.86
EF3	97.51 ± 0.017	7.3±0.060	10.75±0.059	9746.37±1.90

In-vitro drug release study: In vitro drug permeation studies were conducted for ethosomal gel formulations EF1, EF2, and EF3 across a dialysis membrane in a modified Franz diffusion cell, using phosphate buffer pH 7.4 as the receptor medium over a 14-hour study period. Release profiles are summarized in Tables 7 – 10 and illustrated in Figures 2 - 3. The flux of fluconazole through the dialysis membrane substantially exceeded its transport across excised skin, underscoring the rate-limiting barrier function of skin. Release data were analyzed by fitting to zero-order, first-order, Higuchi, and Korsmeyer–Peppas

kinetic models (Table 10; Figures 4 – 5). Zero-order profiles demonstrated reasonably linear behaviour. Korsmeyer–Peppas fitting yielded 'n' exponent values in the range of 0.5 < n < 1.0, consistent with anomalous (non-Fickian) diffusion as the dominant release mechanism. The ethosomal gels provided controlled drug release over 14 hours, whereas no such controlled release profile was observed with the marketed formulation. Drug release from the ethosomal gels ranked in the order: EF2 > EF3 > EF1

In-vitro drug release data of ethosomal gel formulation

Table 7: In-vitro drug release data for F1 (Marketed Fluconazole gel, ZoconTransgelR)

Time (h)	Square Root of Time (h)1/2	Log Time	Cumulative* % Drug Release	Log Cumulative % Drug Release	Cumulative % Drug Remaining	Log Cumulative % Drug Remaining
1	1	0	3.629 ±0.072	0.559	96.371	1.983
2	1.414	0.301	6.314 ±0.101	0.801	93.686	1.971
3	1.732	0.477	13.914±0.271	1.143	86.086	1.934
4	2.000	0.602	19.857±0.289	1.297	80.143	1.903
6	2.449	0.778	30.657±0.459	1.486	69.343	1.841
8	2.828	0.903	45.687±0.514	1.659	54.313	1.734
12	3.464	1.079	56.712±0.915	1.753	43.288	1.636
14	3.742	1.146	62.783±0.961	1.797	37.217	1.570

*Average of three readings

Table 8: In-vitro drug release data for EF1

Time (h)	Square Root of Time(h)1/2	Log Time	Cumulative* % Drug Release	Log Cumulative % Drug Release	Cumulative % Drug Remaining	Log Cumulative % Drug Remaining
1	1	0	8.229±0.095	0.915	91.771	1.963
2	1.414	0.301	15.086 ±0.203	1.179	84.914	1.929
3	1.732	0.477	26.971 ±0.439	1.431	73.029	1.863
4	2.000	0.602	34.286 ±0.586	1.535	65.714	1.818
6	2.449	0.778	44.800 ±0.896	1.651	55.200	1.742
8	2.828	0.903	52.800 ±0.956	1.723	47.200	1.674
12	3.464	1.079	64.320 ±1.154	1.808	35.680	1.552
14	3.742	1.146	76.800 ±1.342	1.885	23.200	1.365

*Average of three readings

Table 9: In-vitro drug release data for EF2

Time (h)	Square Root of Time (h)1/2	Log Time	Cumulative* % Drug Release	Log Cumulative % Drug Release	Cumulative % Drug Remaining	Log Cumulative % Drug Remaining
1	1	0	9.600 ±0.112	0.982	90.400	1.956
2	1.414	0.301	22.857±0.413	1.359	77.143	1.887
3	1.732	0.477	32.000±0.625	1.505	68.000	1.833

4	2.000	0.602	43.429±0.756	1.638	56.571	1.753
6	2.449	0.778	50.286±0.915	1.701	49.714	1.696
8	2.828	0.903	69.600±1.114	1.843	30.400	1.483
12	3.464	1.079	80.160±1.213	1.904	19.840	1.298
14	3.742	1.146	94.080±1.765	1.973	5.920	0.772

*Average of three readings

Table 10: In-vitro drug release data for EF3

Time (h)	Square Root of Time (h)1/2	Log Time	Cumulative * % Drug Release	Log Cumulative % Drug Release	Cumulative % Drug Remaining	Log Cumulative % Drug Remaining
1	1	0	9.143±0.115	0.961	90.857	1.958
2	1.414	0.301	15.920±0.296	1.283	98.080	1.992
3	1.732	0.477	28.800±0.456	1.459	71.200	1.852
4	2.000	0.602	37.029±0.512	1.569	62.971	1.799
6	2.449	0.778	48.457±0.812	1.685	51.543	1.712
8	2.828	0.903	63.840±1.146	1.805	36.160	1.558
12	3.464	1.079	76.320±1.214	1.883	23.680	1.374
14	3.742	1.146	87.840±1.412	1.944	12.160	1.085

*Average of three readings

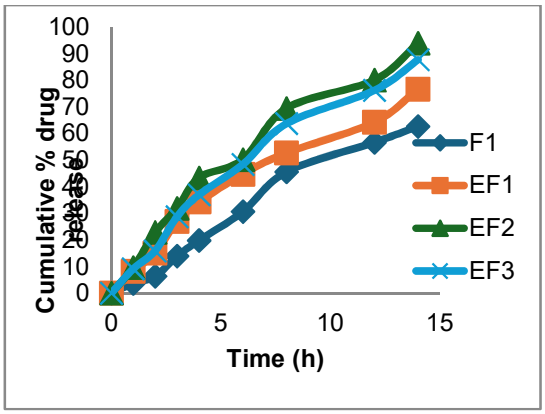

Figure 2: Cumulative %t drug released Vs Time

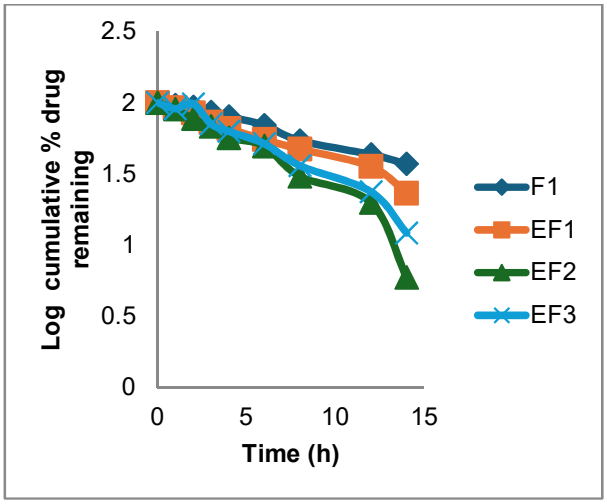

Figure 3. Log cumulative % drug remaining Vs Time

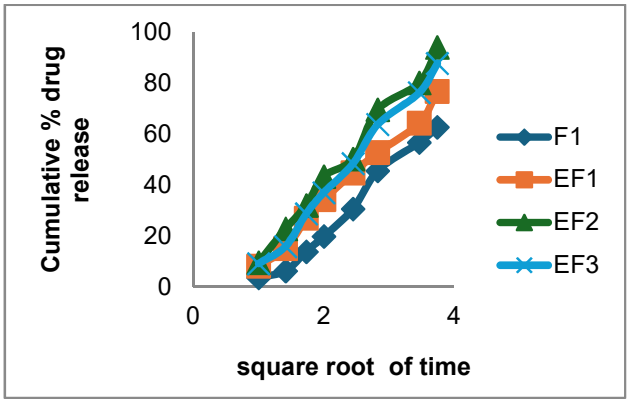

Figure 4. Cumulative % drug released Vs Square root of Time

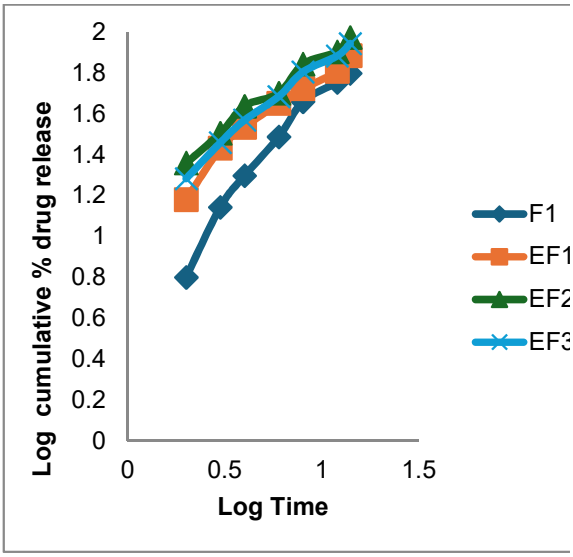

Figure 5. Log cumulative % drug released Vs log Time

Table 11: Regression analysis data of ethosomal gel formulation

Batch	Zero Order		First Order		Higuchi's Model		Korsmeyers Peppas Equation	
	K0 (mg.h-1)	R^2	K1 (h-1)	R^2	Kh (mg.h-1/2)	R^2	n	R^2
F1	6.470	0.903	-0.332	0.863	30.18	0.835	0.670	0.914
EF1	5.195	0.985	-0.071	0.911	21.41	0.868	0.828	0.926
EF2	6.394	0.956	-0.076	0.939	26.38	0.896	0.818	0.989
EF3	6.406	0.913	-0.076	0.931`	25.94	0.908	1.168	0.906

Transmission Electron Microscopy (TEM): TEM operates by directing a focused electron beam through an ultra-thin sample, generating a high-resolution image from the transmitted electrons. The resulting image is magnified and recorded on a detector such as a fluorescent screen, photographic film, or a CCD camera (Donatella et al., 2005).TEM achieves substantially higher spatial resolution than optical microscopy, owing to the short de Broglie wavelength of the electron beam, enabling structural characterization at the atomic level. It is widely used across physical and biological research disciplines. TEM morphological analysis of the ethosomal formulation confirmed a predominantly spherical vesicle geometry (Figure 5.20). Minor heterogeneity in size distribution was noted, possibly related to charge neutralization variability between oppositely charged lipid moieties during vesicle formation at defined pH.TEM imaging further confirmed that the ethosomes formed multilamellar vesicular structures with mean diameters between 100 and 300 nm. The slightly non-spherical morphology observed in some vesicles indicates a degree of membrane flexibility, attributed to the fluidizing effect of ethanol on the vesicle bilayer.

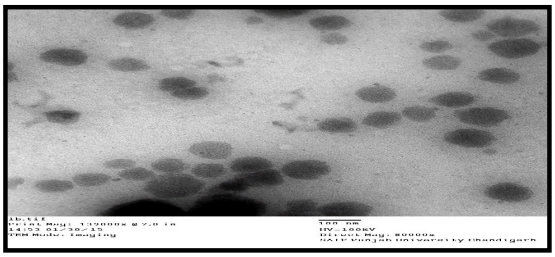

Figure 6: TEM image of ethosome

Evaluation of Liposomal Gel: The liposomal gel formulations were characterized for drug content, pH, Spreadibility, and viscosity, with all results compiled in Table 12.

Drug content: Adequate drug retention is an essential quality criterion for liposomal formulations. Drug content assay of the prepared liposomal gels yielded values ranging from 97.30 to 98.18%, indicating satisfactory encapsulation and retention capacity.

pH: In transdermal formulation development, pH compatibility with skin physiology is a fundamental requirement. The prepared liposomal gels recorded pH values of 6.8–7.1, lying within the physiologically acceptable range for topical application.

Spreadibility: Spreadibility of the liposomal gels

was determined using a modified apparatus based on slip-and-drag measurement. Values ranged from 10.88 to 11.70 g/cm/sec, indicating appropriate consistency for smooth topical administration without excessive resistance or uncontrolled flow.

Viscosity measurements: Viscosity of the liposomal gels was evaluated using a Brookfield DV-II viscometer with a helipath T-Bar spindle for accurate, repeatable measurements. All variables known to affect gel rheology—temperature, pressure, and sample volume—were maintained at constant values throughout testing. Measurements were performed at 25°C, as higher temperatures reduce gel viscosity. Shear rate and measurement duration were the only varied parameters. Samples were equilibrated to room temperature prior to analysis to prevent anomalously high viscosity readings attributable to cold-storage effects.The best method for the selection of spindle was trial and error starting from T91 spindle. Spindles in increasing number were used depending on the % torque and error. The goal is to obtain a viscometer dial or display (% torque) reading between 10 & 100, the relative error of measurement improves as the reading approaches 100. Spindle T 95 was found to be suitable and was used for the measurement of viscosity of all the gels. The Helipath T- Bar spindles were rotated up and down in the sample giving variable viscosities at a number of points programmed over the time. Five readings taken over a period of 60 seconds were averaged to obtain viscosity.

The results show that the viscosity of the gels increased with an increase in polymer concentration. The increase in viscosity with the polymer concentration may be due to increase in bonds between the polymer molecules which lead to formation of a hard and dense compact mass. This may also be due to less amount of liquid in gels with high polymer concentration as compared to gels of low polymer concentration or in other words it can be said the higher the polymer concentration more shear stress if required to produce a specified rate of shear.

Table 12: Results of liposomal formulations

Code	Drug content (%)	pH	Spreadibility (gm/cm/sec.)	Viscosity (cps)
LF1	97.30 ±0.024	7.0±0.021	10.88±0.081	7480±1.15
LF2	97.74±0.020	6.8±0.070	11.70±0.053	10540±1.70
LF3	98.18 ±0.021	7.1±0.050	11.20±0.062	9582±2.05

In-vitro drug release study: Permeation studies for liposomal gel formulations LF1, LF2, and LF3 were conducted using a modified Franz diffusion cell with a dialysis membrane in phosphate buffer pH 7.4 over a 14-hour study period. Data are summarized in Tables 12 and Figures 7 - 9. The permeation rate of fluconazole through the dialysis membrane exceeded its flux across skin, confirming the barrier function of the cutaneous tissue. Release kinetics were analyzed using zero-order, first-order, Higuchi, and Korsmeyer–Peppas models (Table 13 – 15; Figures 7 – 9). Zero-order plots showed reasonably linear profiles. Korsmeyer–Peppas analysis yielded 'n' values between 0.5 and 1.0, consistent with anomalous (non-Fickian) diffusion as the predominant transport mechanism. Drug release from the liposomal gels followed the rank order: LF1 < LF2 < LF3.

In-vitro drug release data of liposomal gel formulation

Table 13. In-vitro drug release data for LF1

Time (h)	Square root of Time (h)1/2	Log Time	Cumulative* % Drug Release	Log Cumulative* % Drug Release	Cumulative % Drug Remaining	Log Cumulative % Drug Remaining
1	1	0	8.229 ±0.154	0.915	91.771	1.963
2	1.414	0.301	14.171±0.197	1.151	85.829	1.934
3	1.732	0.477	25.143±0.581	1.400	74.857	1.874
4	2.000	0.602	33.829±0.597	1.529	66.171	1.821
6	2.449	0.778	40.686±0.764	1.609	59.314	1.773

8	2.828	0.903	50.400±0.896	1.702	49.600	1.695
12	3.464	1.079	56.160±0.945	1.749	43.840	1.642
14	3.742	1.146	66.240±1.114	1.821	33.760	1.528

*Average of three readings

Table 14. In-vitro drug release data for LF2

Time (h)	**Square root of Time (h)1/2**	**Log Time**	**Cumulative * % Drug Release**	**Log Cumulative % Drug Release**	**Cumulative % Drug Remaining**	**Log Cumulative % Drug Remaining**
1	1	0	6.857±0.112	0.836	93.143	1.969
2	1.414	0.301	12.343±0.196	1.091	87.657	1.943
3	1.732	0.477	20.571±0.212	1.313	79.429	1.900
4	2.000	0.602	31.086±0.345	1.493	68.914	1.838
6	2.449	0.778	39.314±0.487	1.595	60.686	1.783
8	2.828	0.903	49.440±0.631	1.694	50.560	1.704
12	3.464	1.079	57.120±1.012	1.757	42.880	1.632
14	3.742	1.146	67.200±1.117	1.827	32.800	1.516

*Average of three readings

Table 15. In-vitro drug release data for LF3

Time (h)	**Square root of Time (h)1/2**	**Log Time**	**Cumulative * % Drug Release**	**Log Cumulative % Drug Release**	**Cumulative % Drug Remaining**	**Log Cumulative % Drug Remaining**
1	1	0	16.457±0.216	1.216	83.543	1.922
2	1.414	0.301	26.514±0.297	1.423	73.486	1.866
3	1.732	0.477	31.543±0.367	1.499	68.457	1.835
4	2.000	0.602	44.800±0.489	1.651	55.200	1.742
6	2.449	0.778	50.286±0.681	1.701	49.714	1.696
8	2.828	0.903	60.800±0.915	1.784	39.200	1.593
12	3.464	1.079	64.457±1.104	1.809	35.543	1.551
14	3.742	1.146	70.400±1.171	1.848	29.600	1.471

*Average of three readings

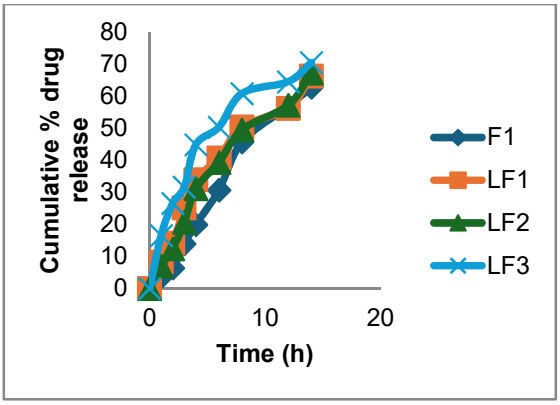

Figure 7. Cumulative % drug released Vs Time

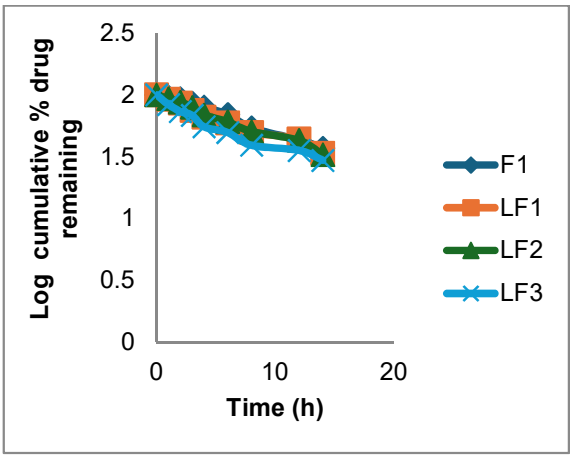

Figure 8. Log cumulative % drug remaining Vs Time

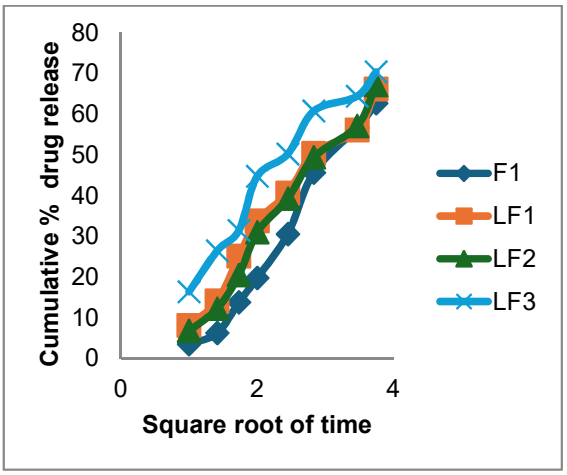

Figure 9. Cumulative percent drug released Vs Square root of Time

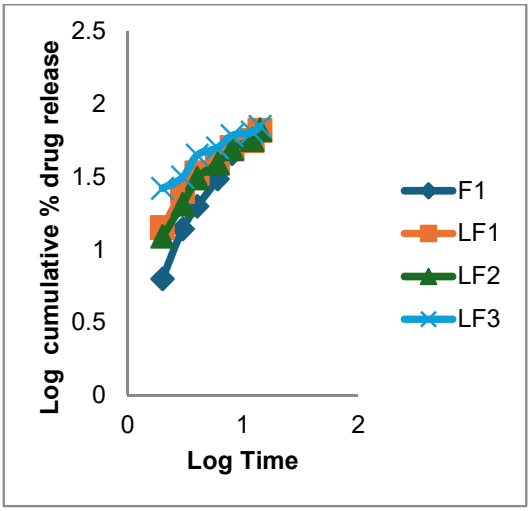

Figure 10. Log cumulative percent drug released Vs Log Time

Table 16. Regression analysis data of liposomal gel formulation

Batch	Zero Order		First Order		Higuchi's Model	Korsmeyers Peppas Equation		
	K0 (mg.h-1)	R^2	K (h-1)	R^2	Kh (mg.h-1/2)	R^2	n	R^2
F1	6.470	0.688.	0.332	0.522	30.18	0.835	0.670	0.992
LF1	4.462	0.928	0.071	0.970	18.68	0.969	0.783	0.964
LF2	4.480	0.859	0.076	0.945	19.58	0.977	0.549	0.969
LF3	4.670	0.953	0.076	0.962	19.22	0.960	0.870	0.974

Table 17. Cumulative percent drug release of optimized batch of ethosome and liposome

Time(h)	Cumulative (%) drug release		
	Fluconazole Gel F1	Ethosomal Gel EF2	Liposomal Gel LF3
1	3.629±0.413	9.600±0.392	16.457±0.483
2	6.314±0.595	22.857±0.463	26.514±0.596
3	13.914±0.287	32.000±0.557	31.543±0.338
4	19.857±0.552	43.429±0.613	44.800±0.472
6	30.657±0.376	50.286±0.427	50.286±0.597
8	45.687±0.441	69.600±0.529	60.800±0.372
12	56.712±0.624	80.160±0.293	64.457±0.491
14	62.783±0.483	94.080±0.436	70.400±0.679

Comparison of optimized formulation with marketed product: The comparative evaluation was conducted against the commercial reference product Zocon Transgel (fluconazole gel 0.5% w/w, Proxima/FDC Limited). At the end of the 14-hour study, cumulative drug release from the marketed gel, optimized ethosomal gel (EF2), and optimized liposomal gel (LF3) amounted to 62.783%, 94.080%, and 70.400%, respectively. The ethosomal formulation demonstrated the highest overall drug permeation, surpassing both the

liposomal gel and the marketed product. The observed release order was: Ethosomal Gel > Liposomal Gel > Marketed Gel.

The superior penetration performance of ethosomal formulations is partly attributable to the known skin permeation-enhancing properties of ethanol. The data indicate a positive correlation between ethanol concentration and drug release rate, with higher ethanol content facilitating greater fluconazole permeation from the ethosomal matrix.

The enhanced skin delivery achieved by ethosomes relative to liposomes is attributed to a synergistic interplay among ethanol, the vesicle carrier, and stratum corneum lipids. A two-stage mechanism has been proposed: ethanol first interacts with polar head groups of stratum corneum lipids, lowering their phase transition temperature and increasing membrane fluidity. This is followed by an 'ethosome effect,' in which deformable vesicles fuse with skin lipids, creating new permeation pathways and enabling delivery to deeper skin layers. Ethanol also imparts membrane flexibility that facilitates deeper tissue penetration, and transdermal drug absorption is driven by fusion events between ethosomes and skin lipids throughout the permeation pathway (El sayed et al., 2006).

Transmission Electron Microscopy: TEM characterization confirmed the formation of small, spherical liposomal vesicles with phospholipid bilayer architecture. Some degree of size distribution variability was noted, possibly attributed to inconsistencies in electrostatic charge neutralization between oppositely charged lipid species during vesicle assembly at the specified pH.TEM further confirmed that the liposomal vesicles exhibited phospholipid bilayer structures with mean diameters of 100–500 nm. The polymeric coating material was visible both encasing individual vesicles and forming bridges between adjacent ones, resulting in the formation of vesicle aggregates.

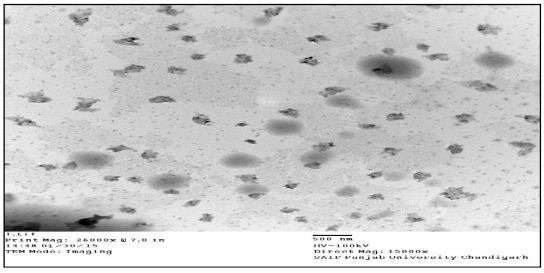

Figure 11. TEM image of liposome

Result of stability studies: The optimized formulations LF3 and EF2 were subjected to stability assessment at two storage temperatures (4.0 ± 0.5°C and 28 ± 0.5°C) over four weeks. No significant changes in physical appearance, vesicle size, or drug content were recorded for either formulation, as documented in Tables 18 –21.

Table 18. Effect of storage temperature on the vesicle size of drug loaded liposomal gel LF3

Time (Days)	Average Vesicle Size (nm)	
	4.0 ± 0.5°C	**28 ± 0.5ºC**
0	320.421± 2.134	320.421± 2.134
7	320.283 ± 3.352	320.532 ± 3.138
14	320.169 ± 4.121	319.232 ± 5.748
21	319.447 ± 3.465	319.116 ± 6.225
28	319.281 ± 4.334	318.531 ± 4.117

*Average of 03 readings

Table 19. Effect of storage temperature on the % drug content of loaded liposomal gel

Time (Days)	Drug Content (%)	
	4.0 ±1°C	**28 ± 1ºC**
0	98.181 ± 0.020	98.181 ± 0.020
7	97.864± 0.124	98.050 ± 0.123
14	97.426± 0.256	97.456 ± 0.458
21	97.114 ± 0.421	97.014 ± 0.754
28	96.954 ± 0.411	96.425 ± 0.412

*Average of 03 readings

Table 20. Effect of storage temperature on the particle size of drug loaded ethosomal gel

Time (Days)	Average Vesicle Size (nm)	
	4.0 ± 0.5°C	**28 ± 0.5°C**
0	367.537 ± 3.138	367.537 ± 3.138
7	366.141± 3.364	364.672 ± 3.107
14	365.234 ± 4.106	365.132 ± 5.713
21	364.892 ± 3.441	366.248 ± 6.284
28	364.326 ± 4.383	366.421 ± 4.153

*Average of 03 readings

Table 21. Effect of storage temperature on the drug content of loaded ethosomal gel EF2

Time (Days)	Drug Content (%)	
	4.0 ±0.5°C	28 ± 0.5°C
0	98.120 ± 0.021	98.120 ± 0.021
7	97.917± 0.575	98.083± 0.158
14	97.265 ±0.279	97.692 ± 0.573
21	97.119 ± 0.265	97.096 ± 0.875
28	97.086 ± 0.887	96.852 ± 0.745

*Average of 03 readings

Antifungal activity of ethosomal and liposomal gel

Microbial cultures: Standardized microbial strains sourced from the Microbial Culture Collection (MCC), National Centre for Cell Science, Pune, Maharashtra, were used to evaluate antifungal activity. Lyophilized cultures were revived by incubation in nutrient and potato dextrose broth at 37 ± 0.5°C for 48 hours, yielding viable cell suspensions. Sub-cultures were established on agar plates under identical conditions to produce pure colonies, which were stored at 4°C as working stock cultures.

Antifungal studies: Lawn cultures of the test pathogens were prepared and screened for susceptibility to each antifungal gel formulation at a concentration of 100 mg/ml using the standard disc diffusion method.

Antifungal activity: Fluconazole effectively inhibited both *Aspergillus niger* and *Candida albicans* at all concentrations tested (20, 50, and 100 mg/ml), confirming its suitability as the reference antifungal agent. The zone of inhibition results are summarized in Tables 22 and 23.

Table 22. Antifungal activity of different gel formulations against Aspergillus niger

Sample	Zone of Inhibition (mm)		
	20mg/ml	50 mg/ml	100mg/ml
Marketed Fluconazole Gel	17±0.22	21±0.12	25±0.11
Ethosomal Gel	16±0.15	24±0.23	29±0.25
Liposomal Gel	16±0.12	22±0.10	27±0.20

Table 23. Antifungal activity of different gel formulations against Candida albicans

Sample	Zone of inhibition (mm)		
	20mg/ml	50 mg/ml	100mg/ml
Marketed Fluconazole Gel	15±0.20	20±0.15	25±0.13
Ethosomal Gel	17±0.11	24±0.21	29±0.20
Liposomal Gel	16±0.12	21±0.13	27±0.27

All three gel formulations—ethosomal, liposomal, and marketed—exhibited antifungal activity against both *Aspergillus niger* and *Candida albicans*, with zones of inhibition ranging from 17 to 29 mm (Figure 12).

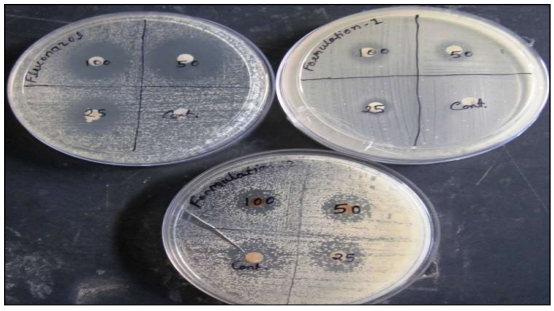

Figure 12. Photograph showing antifungal activity

Comparative evaluation demonstrated that the ethosomal gel produced significantly larger inhibition zones against both Aspergillus niger and Candida albicans than either the liposomal gel or the marketed fluconazole preparation, indicating superior antifungal efficacy.

References

1. Kim, Y. H., Song, C. K., Jung, E., Kim, D. H., & Kim, D. D. (2014). A microemulsion-based hydrogel formulation containing voriconazole for topical skin delivery. *Journal of Pharmaceutical Investigation*, *44*(7), 517-524.

2. Nair, P. M. N. (2017). *Formulation and Physicochemical Characterization of Diethylaminoethyl Dextran Coated Liposome as a Drug Carrier and its Effect on the Rheological Properties of Carbopol Gel* (Doctoral dissertation, University of Malaya (Malaysia)).
3. Negi P, Aggarwal M, Sharma G, Raza K, Singh B, Katare OP. Topical ethosomal emulgel of naproxen using design of experiment. Drug Dev Ind Pharm. 2015;41(11):1838-1847
4. Khan, B. A., Ahmad, N., Alqahtani, A., Baloch, R., Rehman, A. U., & Khan, M. K. (2024). Formulation development of pharmaceutical nanoemulgel for transdermal delivery of feboxostat: physical characterization and in vivo evaluation. *European Journal of Pharmaceutical Sciences*, *195*, 106665.
5. Bhalaria, M. K., Naik, S., & Misra, A. N. (2009). Ethosomes: a novel delivery system for antifungal drugs in the treatment of topical fungal diseases. *Indian journal of experimental biology*, *47*(5), 368-375.
6. Sabale V, Kunjwani H, Sabale P. Formulation and in vitro evaluation of the topical antiageing preparation of the fruit of Benincasa hispida. J Ayurveda Integr Med. 2011 Jul;2(3):124-8. doi: 10.4103/0975-9476.85550.
7. Rai, M., Golińska, P., Sionkowska, A., Shirsat, S., Gade, A. K., Ingle, A. P., ... & Prokisch, J. (2025). Theranostic nanomaterials for scalp and hair fungal infections: advancing diagnosis and treatment amidst challenges. *Expert Review of Anti-infective Therapy*, *23*(8), 617-638.
8. Elsayed, M. M., Abdallah, O. Y., Naggar, V. F., & Khalafallah, N. M. (2007). Lipid vesicles for skin delivery of drugs: reviewing three decades of research. *International journal of pharmaceutics*, *332*(1-2), 1-16.
9. Jeong H, Lee JH, Kim C, Kim JU. Cyclosporine A ethosomes and skin penetration depth using confocal laser scanning microscopy. Pharmazie. 2010;65(6):406-412.
10. Kanwar N, Kulkarni GT, Bhatt S, Bansal K, Sahu SK. Nanoethosome gel of fluconazole using cold homogenization and 3^2 full factorial design. IJPSR. 2019;10(8):3629-3640.
11. Kaur IP, Kakkar S. Topical delivery of antifungal agents and novel nanotechnological approaches. Drug Discov Today. 2010;15(23-24):1032-1040.
12. Kausar H, Mujeeb M, Ahad A, et al. Optimization of ethosomes for topical thymoquinone delivery using Box-Behnken Design. J Drug Deliv Sci Technol. 2019;49:177-184.
13. Hashem, S. M., Gad, M. K., Anwar, H. M., Saleh, N. M., Shamma, R. N., & Elsherif, N. I. (2022). Itraconazole-Loaded Ufasomes: Evaluation, Characterization, and Anti-Fungal Activity against *Candida albicans*. *Pharmaceutics*, *15*(1), 26. https://doi.org/10.3390/pharmaceutics15010026Khan S, Nazim S, Bonde GV, Patel A, Upadhyay S. Itraconazole-loaded ethosomes using QbD for topical antifungal therapy. Drug Deliv. 2020;27(1):180-189.
14. Chavan, A., Daniel, K., & Patel, A. M. (2022). In-silico Exploration of Phytoconstituents of Gymnema sylvestre as Potential Glucokinase Activators and DPP-IV Inhibitors for the Future Synthesis of Silver Nanoparticles for the Treatment of Type 2 Diabetes Mellitus. *Current Enzyme Inhibition*, *18*(1), 47-60.
15. Kumar, S., Kamboj, S., & Saini, V. (2004). Transdermal drug delivery system: A review. *International Journal of Pharmaceutical Sciences Review and Research, 5*(2), 35–45.
16. Kumar A, Kushwaha A. Fluconazole cubosomes for topical antifungal therapy with in vivo evaluation. J Drug Deliv Sci Technol. 2018;46:46-57.
17. Zare-Khafri, M., Alizadeh, F., Nouripour-Sisakht, S., Khodavandi, A., & Gerami, M. (2020). Inhibitory effect of magnetic iron-oxide nanoparticles on the pattern of expression of lanosterol 14α-demethylase (ERG11) in fluconazole-resistant colonising isolate of Candida albicans. *IET nanobiotechnology*, *14*(5), 375-381.